Astronomy
&
Astrophysics

Accurate $V \sin i$ measurements in M 67: The angular momentum evolution of 1.2 $M_\odot$ stars⋆

C. H. F. Melo[1], L. Pasquini[2], and J. R. De Medeiros[3]

[1] Observatoire de Genève, des Maillettes 51, 1290 Sauverny, Switzerland
[2] European Southern Observatory, Karl-Schwarzschild-Strasse 2, 85748 Garching bei München, Germany
[3] Departamento de Física, Universidade Federal do Rio Grande do Norte, 59072-970, Natal, RN, Brazil

Abstract. By using FEROS spectrograph commissioning observations, we build a calibration of the FEROS cross-correlation function (CCF) to determine accurate projected rotational velocities $V \sin i$ for slow rotating F-K dwarf and giant stars. We apply this calibration to a sample of 28 main sequence, turnoff and giant stars belonging to the old open cluster M 67. We find that the stars behave in a very regular manner, depending on their position in the Color-Magnitude (C-M) diagram. Early main sequence G stars have a rotational velocity two times larger than the Sun, and they show a possible trend with $(B-V)$ color, in that redder colors correspond to lower $V \sin i$. The stars at the turnoff are the fastest rotators, with $V \sin i$ between 6.3 and 7.6 km s^{-1}, while stars just above the turn-off are already significantly slower , with values between 4.6 and 4.9 km s^{-1}. Along the Red Giant Branch (RGB), rotation decreases smoothly and for stars above $(B-V) \gtrsim 1$, only upper limits can be found, including for 4 clump stars. Analyzing the angular momentum history of 1.2 $M_\odot$ stars with the help of theoretical evolutionary tracks, we see that these stars probably obey different angular momentum evolution laws on the main sequence and along the RGB: while on the main sequence some extra braking is required in addition to angular momentum conservation, along the RGB the data are well represented by the $I\Omega = C$ law. Finally, comparing the $V \sin i$ of the M 67 turnoff stars with their main sequence progenitors in the younger open clusters NGC 3680 and Hyades we find that the younger clusters show substantially higher rotation rates. This indicates that 1.2 $M_\odot$ stars do experience main sequence braking. This could be relevant also for the interpretation of the nature of the "Lithium gap".

Key words. stars: rotation – stars: interior – open clusters and associations: individual: M 67

1. Introduction

Stellar rotation is a relevant parameter in modern stellar astrophysics: not only is it crucial for our understanding of stellar chromospheric and coronal activity (see e.g. Noyes et al. 1984; Pallavicini et al. 1981), but also, the evolution of stellar angular momentum has been advocated as the mechanism responsible to explain mixing and dilution observations that cannot be otherwise reproduced in the context of "standard" (i.e. non rotating) stellar evolutionary models (Charbonnel & Talon 1999; Deliyannis et al. 2000). As another example, the discovery of fast rotating Horizontal Branch (HB) stars in globular clusters may have deep impact on our understanding of stellar interior structure (Peterson et al. 1985). Finally, we can expect that, once fully consistent rotating models are developed, they will have to satisfy not only the

Color-Magnitude (C-M) diagrams and the abundance patterns observed, but also the observed evolution of the stellar angular momentum.

On the other hand, rotational velocity in late type stars is a quantity which, despite its relevance, has often been neglected. The main reason is that old cool stars, either on the main sequence or evolved, tend to rotate very slowly (of the order of a few km s^{-1}) and the direct measurement of $V \sin i$ is therefore a difficult task, which either requires very high resolution, high S/N observations (e.g. Gray 1976) or long term campaigns to determine rotational periods thanks to the modulation in the core of chromospheric lines induced by the migration of surface inhomogeneities on the stellar surface (see e.g. Baliunas & Vaughan 1985).

It is therefore of prime relevance to measure stellar rotation, not only for many field stars (see e.g. De Medeiros & Mayor 1999; Do Nascimento et al. 2000), but also in stars belonging to open and globular clusters. In these objects, in fact, in addition to the well known advantage of

---

dealing with well determined samples, between the stars located at the turn-off and the giants the difference in stellar masses is small enough that we can to a first approximation consider all these stars as having the same main sequence mass, and therefore to represent an iso-mass evolutionary sequence.

On the observational side, the difficult technical aspects of the $V \sin i$ determination can be solved by using cross-correlation (CCF) techniques (see e.g. Benz & Mayor 1984), provided that:

1. The spectrograph used has a stable Point Spread Function (PSF);
2. Calibrators exist, with $V \sin i$ accurate measurements obtained with other techniques, either with measured periods or with Fourier analysis.

On the other hand, the CCF technique has the big advantage that, once calibrated, clean CCF profiles can be obtained with relatively low S/N ratios ($S/N \sim 10$ or less), therefore allowing the measurements of $V \sin i$ for large samples or for faint stars, for which the determination would be virtually impossible unless very large telescopes are used.

In this work we build and present the calibration for the FEROS spectrograph (Kaufer et al. 1999) and we apply it to a sample of stars belonging to the old open cluster M 67 (Montgomery et al. 1993) which is a very interesting cluster, being one of the oldest open clusters known, with an age of about 4 Gyrs and a turnoff mass of $\sim$1.2 $M_\odot$ (Carraro et al. 1996). M 67 is very well studied, for proper motion membership (Girard et al. 1989), photometry (Montgomery et al. 1993) and investigated for radial velocity binary search (Mathieu et al. 1990, 1992). In addition, via high resolution spectroscopy chemical composition (which resulted very close to solar, Shetrone et al. 2000), Li abundances (Pasquini et al. 1997; Deliyannis et al. 2000), chromospheric activity along the RGB (Dupree et al. 1999), X-ray emission (Pasquini & Belloni 1998) have been investigated.

In Sect. 2 the observations and the sample are discussed; in Sect. 3 the calibration is derived, while Sect. 4 is devoted to the M 67 results. Section 5 summarizes our conclusions.

2. Observations

In the last months of 1998 the FEROS spectrograph was commissioned at the 1.52 m ESO telescope at La Silla (Kaufer et al. 1999). During the two separate commissioning periods, in October and November, several stars with known rotational periods or having very accurate rotational velocities measured with Fourier transform techniques (Gray 1976) were observed, with the scope of investigating if a $V \sin i$ calibration for the FEROS spectrograph could be obtained.

Due to other commissioning tests and to the fact that most of the stars with well determined $V \sin i$ are in the Northern sky, only a limited number of calibrators could

be observed (cf. Table 1). To these, a few stars belonging to another program (Setiawan et al. 2000) were added. These stars are indicated in Table 1.

Unlike other spectrographs to which this technique has been applied, FEROS did not yet have a frozen configuration during commissioning, and some interventions on the spectrograph setup were necessary between the October and November commissioning runs. This was readily traced in our observations: the measured width of the CCF was indeed larger by 0.19 km s^{-1} in October; we could check this by observing the same stars in the two periods, and also because the radial velocity calibrators Tau Cet (HD 10700) and 51 Peg (HD 217014) were observed almost every night. A direct comparison of the CCF widths for these stars confirms exactly what was found for the other objects. Note therefore that the CCF widths given in Table 1 and observed in October have been corrected by this amount (cf. next section).

Since FEROS is not a spectrograph dedicated to a single program, we strongly suggest to the potential users of our calibration to observe in their observing run at least one of the calibrators presented in this paper, in order to ensure that zero point shifts, due to interventions on the spectrograph, have not occurred.

The M 67 observations were all carried out in the second commissioning period (November); the 28 stars were chosen to be proper motion members (Girard et al. 1989), to cover as evenly as possible the M 67 sequence from the turnoff to the tip of the RGB. The stars span a range in magnitude between $m_v \sim 9.7$ to $m_v \sim 14$, and thanks to the high efficiency of the spectrograph, the integration time ranged between $\sim$5 and $\sim$20 min. The integration was set to provide an even distribution of S/N ratios for all the stars, between S/N 10 and 20, although for the brightest objects the S/N ratio could be easily pushed up to 40. We note that HD 10700 was observed every night when the M 67 observations were taken, and the CCF width, σ_{obs} of Tau Cet was extremely constant: 4.476 ± 0.016 km s^{-1}.

The data were reduced using the FEROS pipeline and they were directly downloaded from the public FEROS commissioning database, available on the web (Kaufer et al. 1999). Additional data on the observations, if required can therefore be found directly on the FEROS database at `http://www.ls.eso.org/lasilla/Telescopes/2p2T/E1p5M/FEROS/`. The wavelength binning was the same for all observations, at 0.03 Å/pixel.

3. The $\sigma - V \sin i$ calibration for FEROS

The width (σ) of the cross-correlation function (CCF) of a star results from several broadening mechanisms which depend on, for instance, gravity, turbulence, magnetic fields, effective temperature, metallicity, rotation. In addition, the instrumental profile also contributes to the broadening of the spectrum and therefore to the CCF. Thus, in order to correctly measure the rotational contribution to

the width of the CCF (σ), we should model the contributions of broadening mechanisms other than rotation. For slow rotators ($V \sin i \lesssim 20$ km s^{-1}), the CCF is still very well approximated by a Gaussian. In this case, the rotational broadening will correspond to a quadratic broadening of the CCF, i.e., the measured width of the CCF of a rotating star will be related to the width of the CCF of a non-rotating stars (with otherwise similar characteristics) as follow:

$$\sigma_{\rm obs}^2 = \sigma_{\rm rot}^2 + \sigma_0^2$$

where $\sigma_{\rm obs}$ is the width of the CCF of the star whose rotation we want to measure, $\sigma_{\rm rot}^2$ is the rotational broadening and σ_0^2 is the the width of the CCF of the non-rotating star. σ_0^2 is a function of all the other broadening mechanism (including the instrumental profile) except rotation, and it can be very well expressed as a function of the color and luminosity class of stars. Therefore, the projected rotational velocity $V \sin i$ can be expressed by (Benz & Mayor 1984; Allain 1997; Queloz et al. 1998):

$$V \sin i = A\sqrt{\sigma_{\rm obs}^2 - \sigma_0^2} \qquad (1)$$

where A is a constant coupling the differential broadening of the CCF to the $V \sin i$ of stars. Equation (1) clearly shows the relevance of σ_0 for the measurement of the $V \sin i$ of slow rotators for which $\sigma_{\rm obs} \sim \sigma_0$.

3.1. The coupling constant A

In order to calculate the constant A in Eq. (1), we have proceeded as described in Queloz et al. (1998). We have chosen four slowly rotating stars. Each spectrum was convolved with Gray's (1976) rotational profile for $V \sin i = 5$ up to 15 km s^{-1} and the respective CCF was calculated. Finally A was found for each star by fitting the relation $V \sin i^2$ versus $\sigma_{\rm obs}^2$ by a straight line for which the squared root of the slope gives A. We will adopt the mean value $< A >= 1.9 \pm 0.1$.

3.2. Modeling of σ_0

As we said above, σ_0 is a critical parameter. The measurement of very small $V \sin i$ will be limited by the uncertainty on σ_0 (and on the uncertainties in the measurement of the CCF $\sigma_{\rm obs}$ which will be discussed in the next section). Since the broadening mechanisms are a function of the temperature and gravity, we may expect a smooth dependence for σ_0 as a function of the stellar color and luminosity class, although, in the case of CORAVEL spectrograph (Baranne et al. 1979), no differences were observed between luminosity V and III objects (De Medeiros & Mayor 1999).

In Table 1 we list the observed slowly-rotating stars for which accurate $V \sin i$ are known. These stars have $V \sin i$ either determined by measured rotational periods or by Fourier analysis (Gray 1976). For each of them, σ_0 was determined by using Eq. (1). Then we carried
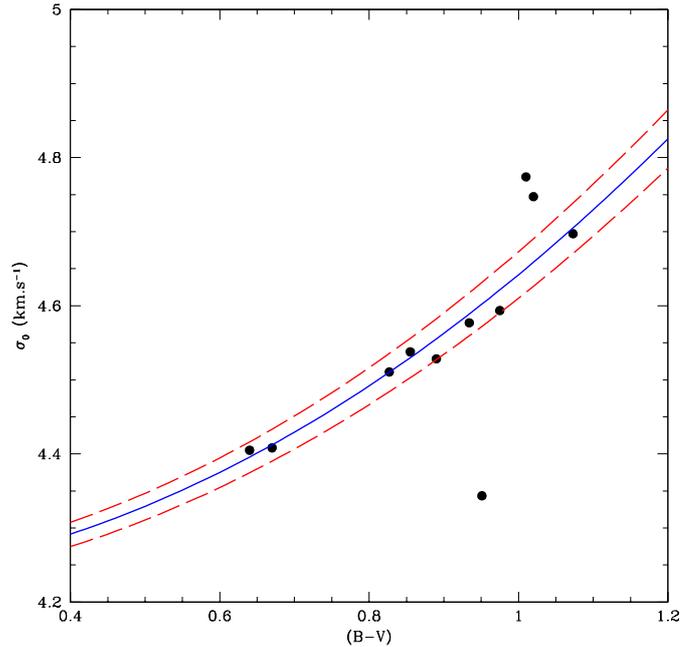

Fig. 1. σ_0 as a function of $(B-V)$ for the calibrators listed in Table 1. The fitted relation (Eq. (2)) is shown as a continuous line. The two dashed lines show the error on the fit. This error sets at 1.3 km s^{-1} the minimum value of $V \sin i$ that can be measured with our calibration (cf. Sect. 3.3).

Table 1. Slow rotators used in the calibration of σ_0 as a function of $(B-V)$. Column 1: HD number; Col. 2: $(B-V)$; Col. 3: Spectral Type; Col. 4: $V \sin i$ from literature; Col. 5: σ_0; Col. 6 $\sigma_{\rm obs}$; Col. 7: $V \sin i$ derived from our calibration and error.

HD	$(B-V)$	ST	$V \sin i$ other	σ_0	$\sigma_{\rm obs}$	$V \sin i$ FEROS
4128	1.02	K0III	3.0^a	4.747	5.003	3.5 ± 0.5
4628	0.890	K2V	0.67^b	4.528	4.542	< 1.3
27371	0.975	K0III	2.4^a	4.594	4.757	2.2 ± 0.6
27697	1.073	K0III	2.5^a	4.697	4.865	2.4 ± 0.6
28305	1.01	K0III	2.5^a	4.774	4.952	3.3 ± 0.5
$113226^\dagger$	0.934	G8III	3.2^c	4.576	4.877	3.1 ± 0.5
149661	0.827	K0V	1.46^b	4.511	4.576	1.5 ± 0.6
155885	0.855	K1V	1.31^b	4.538	4.575	1.3 ± 0.6
$165760^\dagger$	0.951	G8III	3.9^a	4.343	4.804	2.6 ± 0.5
217014	0.67	G2V	2.8^d	4.408	4.624	2.6 ± 0.5
Sun	0.64	G2V	2.0^b	4.405	4.529	2.1 ± 0.5

[a] Gray (1989).
[b] Rotation period taken from Donahue et al. (1996).
[c] Fekel (1997).
[d] Mayor & Queloz (1995).
[†] Taken from Setiawan et al. (2000).

out a least-squared fit of data by the analytical function $\sigma_0 = a_0 + a_2 (B-V)^2$. Since this quadratic dependence of σ_0 on $(B-V)$ has been shown to be successful in the calibration of both instruments, CORAVEL (Benz & Mayor 1984) and ELODIE (Queloz et al. 1998), we decided to adopt the same expression in this work. The quadratic form also allows us to perform a direct comparison and to

scale our results with those found in the case of CORAVEL and ELODIE. Thus, the basis supporting the choice of a squared dependence of σ_0 on $(B-V)$ lies much more in an empirical ground rather than in a theoretical one. In fact, in the range of $(B-V)$ covered by the calibrators listed in Table 1, a linear fit was equally tried, yielding similar results to the quadratic case. In the fit procedure, the weights were arbitrarily chosen as follow: 50 for HD 217014 (51 Peg) and the Sun which are our best points, 30 for stars with two or more observations (HD 27371, HD 27697, HD 155885), in this case the mean $\sigma_{\rm obs}$ of these observations was given, 10 for stars with only one observation (HD 4128, HD 4628, HD 28305, HD 113226, HD 149661) and 5 to highly deviant points (HD 165760).

The σ_0 for three objects, namely, HD 4128 ($B-V = 1.02$, $\sigma_0 = 4.747$), HD 28305 ($B-V = 1.01$, $\sigma_0 = 4.774$) and HD 165760 ($B-V = 0.95$, $\sigma_0 = 4.343$) shows an unexpected deviant behavior. A possible explanation for such a behavior might have to do with the metal content of these stars. Since a rise in metallicity increases the number of saturated lines, the width of the CCF is slightly broadened as well. The inverse is equally true, i.e., a diminution of the stellar metallicity lead to a slightly narrower CCF. Let us check whether this hypothesis may be evoked to account for their deviant behavior. HD 28305 is a Hyades giant, with a super solar metallicity (Fe/H = 0.13, Boesgaard & Friel 1990). According to Taylor (1999), HD 4128 is a slightly richer than the Sun (Fe/H = 0.068) while Cayrel de Strobel et al. (1997) give two different values for the Fe/H of HD 165760, namely, Fe/H = -0.21 and Fe/H = -0.10. Even if the Fe/H measurements are qualitatively consistent with the hypothesis made above, the differences among the metal content of these three stars are too small to account for the observed differences in the $V \sin i$. Clearly, a proper discussion on the metallicity effects can only be done with a larger sample of calibrators having well-determined metallicities.

Even for these three deviant points, the differences between the $V \sin i$ obtained with our calibration and the $V \sin i$ compiled from the literature for HD 4128 and HD 28305 are, respectively, of 0.5 km s^{-1} and 0.8 km s^{-1}, which are well within our errors. Thus, the really deviant point among these three objects is HD 165760 for which our calibration gives a $V \sin i$ of 2.6 km s^{-1} against 3.9 km s^{-1} found by Gray (1989). In this sense, it is worth noticing that the macroturbulence given by Gray (1989) for this object is lower than that found for the other stars in his Table 2 with the same spectral type as HD 165760 (the differences in the macroturbulence measurements range from 0.5 km s^{-1} to 1.6 km s^{-1}). If this difference in the macroturbulence is real, than we cannot use the cross-correlation technique to measure very low $V \sin i$ since one of its basic hypotheses is that stars of same spectral type show a similar intrinsic broadening (i.e., σ_0). On the other hand, there is no apparent physical reason to believe that stars of same luminosity class and having identical spectral types will not show a similar macroturbulence value. This leads us to think that the discrepancy

observed for HD 165760 between our $V \sin i$ and the one computed by Gray may be due to the uncertainties on the Gray's measurement. This hypothesis is partially supported by the $V \sin i$ of HD 165760 given by De Medeiros & Mayor (1999) in their catalog of rotational velocities obtained with CORAVEL for evolved stars. These authors measured a $V \sin i$ of 2.2 km s^{-1} which is very close to that found by us (2.6 km s^{-1}). Let us recall that regardless of the reasons behind this discrepancy, for the 7 other calibrators listed in Table 1, the agreement between our $V \sin i$ and those from the literature is extremely good.

The χ-squared linear fit yields:

$$\sigma_0 = 0.417(B-V)^2 + 4.225. \tag{2}$$

The error on a_0 and a_2 are 0.014 and 0.018, respectively.

The $V \sin i$ calculated using Eqs. (1) and (2) are well in agreement with the $V \sin i$ from the literature. We obtain a rms on the one-to-one relation ($V \sin i_{\rm FEROS} - V \sin i_{\rm other}$) of 0.52 km s^{-1}. Further, we compared our calibration to that obtained by Queloz et al. (1998) for the spectrograph ELODIE (Baranne et al. 1996) which has a resolution slightly lower than FEROS ($R = 42\,000$ for ELODIE and $R = 50\,000$ for FEROS). We rescaled our calibration to ELODIE resolution in order to compare it to Queloz et al. (1998) calibration made for dwarf stars. After the rescaling, our calibration agrees very well with the one of Queloz et al. (1998), we obtained $\sigma_0 = 4.51 + 0.39(B-V)^2$ which is close to $\sigma_0 = 4.51 + 0.27(B-V)^2$ found by Queloz et al. (1998). The rotational projected velocities of our list of calibrators computed using Eq. (2) are given in the last column of Table 1.

3.3. Upper limits estimate

In the regime of slow rotators i.e., $\sigma_{\rm obs} \gtrsim \sigma_0$, the error on the parameters a_0 and a_2 of expression (2) will set the error on the $V \sin i$ measured with our technique. Differentiating Eq. (2) we obtain:

$$\Delta\sigma_0 = \Delta a_2 (B-V)^2 + \Delta a_0 \tag{3}$$

where $\Delta a_0 = 0.014$ and $\Delta a_2 = 0.018$.

Thus $\Delta\sigma_0 = 0.0185$ for $(B-V) = 0.5$ and $\Delta\sigma_0 = 0.04$ for $(B-V) = 1.2$. As we expected to have very low rotation at $(B-V) \gtrsim 1.0$ (i.e., along the RGB and the sub-giant branch, SGB), we will adopt then a conservative value for $\Delta\sigma_0 = 0.05$, independently of $(B-V)$. Let us now evaluate the $V \sin i$ corresponding to this uncertainty on σ_0. For $\sigma_{\rm obs} = \sigma_0 + \epsilon$, where ϵ is a small quantity compared to σ_0, Eq. (1) can be approximated to:

$$V \sin i_{\rm inf} \sim A\sqrt{2\sigma_0\epsilon}. \tag{4}$$

Now taking $A = 1.9$, $\sigma_0 = 4.9$ and $\epsilon = \Delta\sigma_0 = 0.05$ we find $V \sin i_{\rm inf} = 1.3$ km s^{-1}. Thus, for stars having $\sigma \sim \sigma_0$, the values of $V \sin i$ derived with our calibration have an error of the order of $V \sin i_{\rm inf} = 1.3$ km s^{-1}.

3.4. Error estimations

The errors on the radial velocity $V_{\rm r}$ and on the projected rotational velocity $V \sin i$ as a function of the signal-to-noise ratio S/N and as a function of the CCF depth H were estimated by Monte Carlo simulations following the recipes of Dubath et al. (1990) which consists of the following steps: for a fixed S/N, suitable constants were added to a high S/N spectrum in order to play the role of a veiling continuum which renders the final CCF shallower than the original one. The constants were chosen in order to yield CCF with depth of 0.10, 0.15 and 0.20. Following, for a given H, photon and read-out noises were added to our template spectrum in order to mimic a set of low to moderate values of S/N of 1, 2, 3, 5, 10, 15 and 20. For each point $(H, S/N)$, 300 synthetic spectra are built and cross-correlated with the same mask as that used for our program stars. From the resulting CCFs, the radial velocity and the width are measured. The standard deviation ϵ of these two parameters is then calculated using these 300 synthetic measurements. Finally, for each parameter, we find the constants C, α and β which best fit the relation

$$\epsilon = \frac{C}{(S/N)^{\alpha} \times H^{\beta}}. \qquad (5)$$

For the error on the radial velocity we found $C = 0.044$ km s^{-1}, $\alpha = 1.02$ and $\beta = 0.96$. For the error on the $\sigma_{\rm obs}$ we obtained $C = 0.040$ km s^{-1}, $\alpha = 1.02$ and $\beta = 0.94$. The best fit curves are shown as continuous lines in Fig. 2. However, for convenience, we prefer to adopt the relation shown as dashed line,

$$\epsilon(V_{\rm r}) = \epsilon(\sigma_{\rm obs}) = \frac{0.037}{S/N \times H} \left[\text{km s}^{-1} \right]. \qquad (6)$$

Note that Eq. (6) concerns the error on $V_{\rm r}$ due to the photon noise only which for very high S/N will be negligible. In the regime of the highly accurate radial velocities ($\epsilon(V_{\rm r}) \sim 1$ m s^{-1}), the errors will be dominated by the systematic errors due to the stability of the spectrograph (see next section for an estimation of the systematic errors; for a discussion on the subject of precise radial velocity measurements and fundamental photon noise limit see e.g. Bouchy et al. 2001; Marcy & Butler 1992).

Since the error on $\sigma_{\rm obs}$ has been determined, we are ready to estimate the error on our $V \sin i$. Differentiating Eq. (1) we get:

$$|\Delta(V \sin i)|_{\rm mes} = \frac{1.9^2}{V \sin i} \sqrt{|\sigma_{\rm obs} \Delta \sigma_{\rm obs}|^2 + |\sigma_0 \Delta \sigma_0|^2}. \qquad (7)$$

Putting $\Delta \sigma_0 = 0.05$, and substituting Eq. (6) into Eq. (7) we get

$$|\Delta(V \sin i)|_{\rm mes} = \frac{1.9^2}{V \sin i} \sqrt{\left(\frac{0.037}{S/N \times H} \sigma_{\rm obs} \right)^2 + (0.05 \sigma_0)^2} \qquad (8)$$

which is the error due to the uncertainties on the measurement of $\sigma_{\rm obs}$ and σ_0. However, even if $\sigma_{\rm obs}$ and σ_0 could be estimated precisely, we still would have a rms of

0.52 km s^{-1} when comparing our $V \sin i$ with those from the literature. Thus, the total error on $V \sin i$ is:

$$|\Delta(V \sin i)|_{\rm tot} = \sqrt{|\Delta(V \sin i)|_{\rm mes}^2 + 0.52^2}. \qquad (9)$$

4. M 67 Results

The 28 stars observed are given in Table 2, where the photometry from Montgomery et al. (1993) has been adopted for all stars, except for S 989 and S 1001, which are not present in the Montgomery et al. sample. Photometry from Sagar & Pati (1989) and from Sanders (1989) was adopted for S 898 and S 1001, respectively. In Table 2 together with the magnitude and colors, the $\sigma_{\rm obs}$, the retrieved $V \sin i$ and radial velocities are given, with their errors. Note that the radial velocity errors quoted reflect *only* the internal measurement errors, as given in the previous section. Even though FEROS is contained in an enclosure and in a thermally controlled room, small shifts in wavelength in the spectrograph are possible due to temperature and pressure variations, inducing therefore small changes in the zero point of the $V_{\rm r}$. The M 67 observations were not acquired with simultaneous Th-Ar calibrations, nor bracketed by Th-Ar exposures, therefore the zero point shift should be added to the errors quoted in Table 2. In order to quantify this shift we again use the Tau Cet (HD 10700) observations, and found that for this star $V_{\rm r}$ was -16.15 ± 0.15 km s^{-1}. Therefore an uncertainty of 0.15 km s^{-1} should be added to the $V_{\rm r}$ errors in Table 2. Among the objects listed in Table 2, there are three known single-lined spectroscopic binaries (Mathieu et al. 1990), namely, S 986, S 1221 and S 1250. In particular, for S 986 the secondary is seen in the CCF, thus its radial velocity can be combined with the previously known SB1 orbit to yield the secondary minimum mass $M_2 \sin^3 i$. S 1011, S 1064, S 1314 and S 2205 also present a radial velocity inconsistent with the cluster velocity of 33.6 km s^{-1} with an observed velocity dispersion of 0.5 km s^{-1} (Mathieu 1983). For S 1011, S 1064 and S 1314, Jones et al. (1999) also found radial velocities in disagreement with the cluster velocity. In fact, their radial velocities are also different from our radial velocities given in Table 2, which suggests that these three objects are actually spectroscopic binaries. This suspicion grows stronger if we look at the CCFs of the objects listed in Table 2, which are shown in Fig. 3. We see that S 1314 and S 1064 show a double-lined CCF that characterizes these objects as SB2 systems. For S 1011, a small secondary peak is also seen, although less clear than in the latter case. However, no sign of a secondary is seen in CCF of S 2205, which may indicate that this object is a single-lined binary or a non-member.

Let us recall that, except for S 986, none of the known binaries has periods so short as to indicate that possible orbital synchronization could be responsible for modifying the evolution of the angular momentum as a single star. In addition, in order to be able to use Eq. (1) to derive accurate $V \sin i$, the true colors of the object must be known. In the case of a binary system, the observed $(B-V)$ are
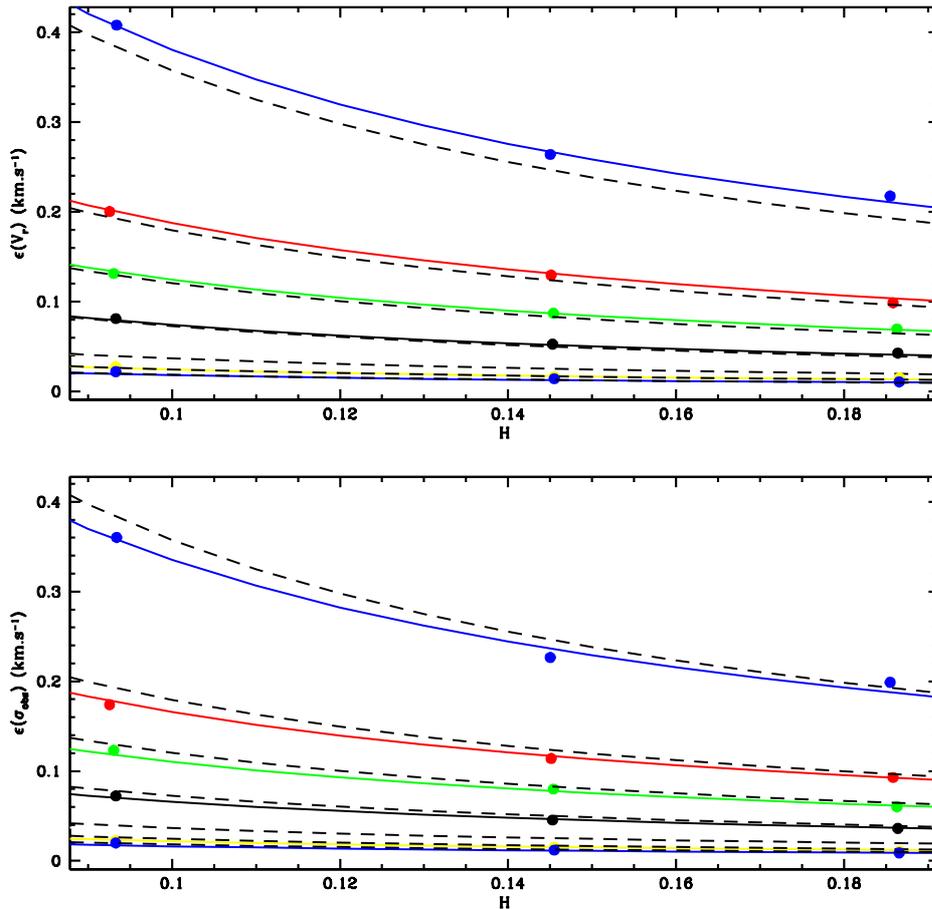
Fig. 2. Monte Carlo simulations to estimate the uncertainties on the measurement of the width of the CCF, $\sigma_{\rm obs}$, and on the measurement of the radial velocity. Each point corresponds to 300 simulations. See text for explanations.

a mixture of the $(B-V)$ of the two components. For a SB1 system, we must assume that the observed $(B-V)$ is totally due to the primary star, since the secondary is not seen in the cross-correlation function, it may not contribute that much to the total light of the system, assuming that the photometry and the spectroscopic share the same wavelength domain. For a SB2 system, $V \sin i$ can be estimated by assuming that both primary and secondary have the same color, which may be correct if the mass ratio q is near of one. On the other hand, if highly accurate $V \sin i$ are desired, true colors must be obtained, for instance, through a spectral fit of the observed spectrum by a synthetic binary spectrum (e.g., Covino et al. 2000). For the binaries and possible binaries listed in Table 2 the observed $(B-V)$ was assumed to be totally due to the primaries.

It is worth noticing that the $V \sin i$ for these binaries and possible binaries are not higher than those of similar single stars, as expected from relatively long period systems which have not suffered strong tidal interactions. Even though we prefer to be conservative and *not* consider these binaries and possible binaries in our discussion.

Note also that for the computation of the $V \sin i$, a color excess of $E(B-V) = 0.05$ for M 67 has been assumed.

In Fig. 4 the color magnitude diagram of the observed stars is shown. The stars are sampled from the main sequence, to the turn-off and the RGB; in addition Five clump giants are easily identified at $(B-V) \sim 1.1$ and $m_v \sim 10.6$.

In this figure the symbols are proportional to the measured $V \sin i$, and this crude representation already shows quite regular patterns associated with different regions of the C-M diagram. In the same figure the evolutionary track for 1.2 $M_\odot$, solar metallicity is shown. The track is from Girardi et al. (2000), who kindly computed the stellar momentum of inertia for each step (see Pasquini et al. 2000). The track represents very well the turnoff region and the subgiants, while it is slightly redder than the observed stars along the RGB.

In Fig. 5, $V \sin i$ as a function of the $(B-V)_0$ color is shown. The data from Table 2 have been corrected by $4/\pi$ to consider the projection effect. Since this figure summarizes most of our results, some detailed discussion of it will be needed.

The first striking aspect is that the stars behave, as far as $V \sin i$ is concerned, in an extremely regular way: in each position of the color-magnitude diagram, they show very similar rotational velocities. This is not the case in most younger clusters, where stars sharing the same
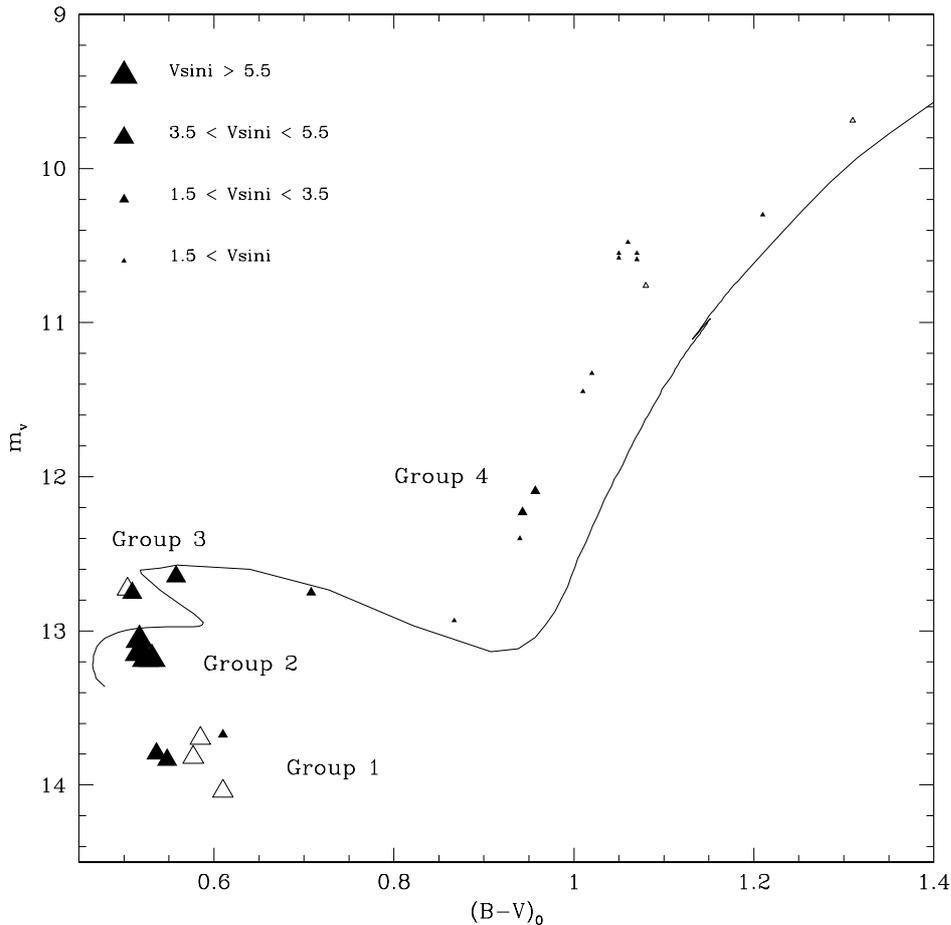
Fig. 3. CCF relative intensity (dots) and the Gaussian fit (solid line) versus radial velocity for M 67 stars observed in this paper. In some cases a small-secondary peak is seen (see text).

Fig. 4. The color magnitude diagram of the observed stars in M 67 is shown. Singles stars are shown as filled triangles, while binaries are represented by empty triangles. Symbols size is proportional to the observed $V \sin i$. Correction for $E(B-V) = 0.05$ has been applied. Overimposed is the 1.2 $M_\odot$ evolutionary track from Girardi et al. (2000) used to compute the stellar momentum of inertia.

position in the C-M diagram may show very different rotation rates.

The 6 main sequence stars (Group 1) below the turnoff (cf. Fig. 4 and Table 2) are given as open triangles. This is a group of early G main sequence stars and their rotational velocities are constrained between 4.3 and 5.8 km s^{-1}. The diagram also suggests that a strong dependence on the stellar color in this small $(B-V)$ range is present, in that the rotational velocity becomes smaller with increasing colors. As these stars have the same age and if we further assume that they started with similar $V \sin i$ on the ZAMS, the cooler ones would slow down a bit more because they possess deeper subphotospheric convective zone. The value of rotational velocity observed is higher that of the Sun, in agreement with the fact that M 67 is younger than the Sun. In this respect, however, we note that these stars are slightly hotter than the Sun, ($\sim$0.05 in $(B-V)$), therefore we do not believe that the mean $< V \sin i >= 4.1$ km s^{-1}, that is about twice the solar $V \sin i$, can be taken yet as a proper comparison value to derive rotation-age dependencies.

Continuing the analysis of the Fig. 5 using Fig. 4 as a guide, the second group (Group 2) is composed by the

4 stars close (but not above) the turn-off. They are more massive than the previous group and they show the highest $V \sin i$ in the whole cluster. They are very similar and have a mean rotational velocity of $\sim$8.5 km s^{-1}. These stars can be considered to be at the edge of the main sequence and represent the turn-off.

A third group (Group 3) is composed of the stars just above the turnoff (3 stars). Again, the rotational velocities for these objects are extremely homogeneous, with values which are almost 50% lower than for the fastest rotators ($\sim$6.0 km s^{-1}). This is quite interesting, because it indicates that in a very small region of the H-R diagram, just after passing the main sequence, the stars are strongly spun down. This region is also very attractive because it is where, according to rotational models, a strong effect on light elements abundances may be visible (Charbonnel & Talon 1999).

Along the subgiant branch rotation tends to slow further, and for stars with $(B-V) \gtrsim 1$ (Group 4) only upper limits can be found, including for the clump stars. This is in qualitative agreement with the simple picture that while evolving, the stars get higher momentum of inertia and therefore spin down (see e.g. Pasquini et al. 2000).
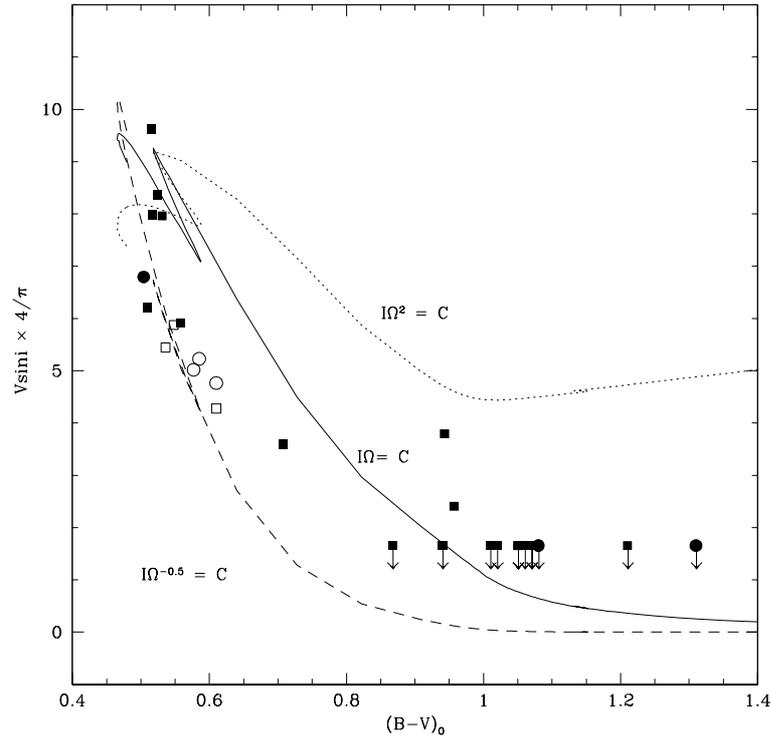
Fig. 5. Rotational velocities vs. $(B-V)_0$ color for the M 67 stars. Open squares (circles) show main sequence single (binary) stars. Filled squares (circles) represent turnoff and evolved single (binary) stars. The different curves represent simple hypotheses on the evolution of angular momentum: $I\Omega = C$ (continuous), $I\Omega^2 = C$ (dotted) and $I\Omega^{0.5} = C$ (dashed).

In their work, based on CORAVEL determination of $V \sin i$, these authors found an intriguing result: for low mass stars in their sample the $V \sin i$ did not show an appreciable decrease along the RGB. With our better defined sample and more accurate $V \sin i$ determination, we see that this effect is not present; but we also analyze here a sample which is slightly more massive than that analyzed by Pasquini et al. (2000). Taken at face value, the M 67 data could suggest a very sudden drop at $(B-V) \sim 1$, and if this was the case it would be interesting to attempt to connect it to special events on the RGB. Our data points are not sufficient to trace this hypothesis.

It is also very interesting to note that the clump stars do not show high rotational velocities, but only upper limits. A possibility to explain these low rotational velocities could be the absence of fast rotating core on the main sequence which was evoked by Peterson (1985) to explain the fast rotation observed in HB stars in some globular clusters.

In essence we can summarize our observational results on the $V \sin i$ evolution of 1.2 $M_\odot$ stars in M 67 by saying that:

1. The stars behave in a very regular way as far as $V \sin i$ is concerned: at each position in the C-M diagram they show similar values of $V \sin i$ (but more stars would help in investigating this point further);
2. Main sequence early G stars (Group 1) have rotational velocity between 4.3 and 5.8 km s^{-1}. There are

indications that rotational velocity decreases with increasing $(B-V)$;
3. Turnoff stars (Group 2) show the highest values of rotational velocity, but a large drop is present as soon as the star evolves out of the turnoff (Group 3);
4. The rotational velocity continues to drop along the subgiant branch (Group 4), by a factor $\sim$2. Only upper limits could be obtained for stars with $(B-V) \gtrsim 1$ and this is also true for the clump stars.

In the following, we would like to better quantify the evolution of the stellar angular momentum for the M 67 stars. In order to do so, we use the momentum of inertia I as computed from the Girardi et al. (2000) tracks (Girardi, private communication, see Pasquini et al. 2000 for details). We have then assumed simple functional laws for angular momentum evolution of the type $I\Omega^\alpha = C$ where C is a constant and $\alpha = 0.5, 1, 2$ and we scale them to match the rotational velocity of the turnoff stars of M 67. Note that this means that $V \sin i \propto R \times I^{-\frac{1}{\alpha}}$. R and I are taken from the evolutionary tracks. These simple laws assume solid body rotation; when $\alpha = 1$ this implies that the angular momentum remains constant along the evolution; $\alpha > 1$ implies transfer of momentum from the interior, while $\alpha < 1$ requires some extra mechanism which tends to brake the rotation beyond what is expected from angular momentum conservation. At the moment these curves can only give semi-quantitative answers, in that, as is clear from Fig. 4 the evolutionary track does not reproduce perfectly the RGB of M 67; this implies that the theoretical

Table 2. FEROS projected rotational velocity $V \sin i$ and radial velocity V_r for M 67 stars observed in this work. Column 1: Sanders (1977) numbers; Col. 2: Visual apparent magnitudes m_v from Montgomery et al. (1993); Col. 3: $(B-V)$ also from Montgomery et al. (1993); Col. 4: σ_{obs}; Col. 5: $V \sin i$ derived from our calibration and error; Col. 6: V_r. Columns 4, 5 and 6 are given in km s^{-1}.

Star	m_v	$(B-V)$	σ_{obs}	$V \sin i$	V_r
Group 1					
S 1011[††]	13.82	0.627	4.831	4.0 ± 0.6	27.228 ± 0.036
S 1055	13.80	0.586	4.892	4.3 ± 0.6	34.316 ± 0.034
S 1064[††]	14.04	0.660	4.802	3.7 ± 0.6	40.572 ± 0.041
S 1075	13.84	0.598	4.982	4.6 ± 0.6	33.609 ± 0.042
S 1256	13.67	0.660	4.723	3.4 ± 0.7	33.606 ± 0.037
S 1314[†]	13.70	0.635	4.873	4.1 ± 0.6	27.108 ± 0.030
Group 2					
S 988	13.18	0.574	5.548	6.6 ± 0.6	34.284 ± 0.026
S 994	13.18	0.581	5.448	6.3 ± 0.6	34.362 ± 0.020
S 998	13.06	0.567	5.447	6.3 ± 0.6	34.644 ± 0.025
S 2205	13.15	0.566	5.884	7.6 ± 0.6	31.253 ± 0.039
Group 3					
S 986[m,†]	12.73	0.554	5.161	5.3 ± 0.6	63.412 ± 0.022
S 995	12.76	0.559	5.037	4.9 ± 0.6	34.538 ± 0.017
S 1034	12.65	0.608	4.992	4.6 ± 0.6	34.468 ± 0.017
Group 4					
S 989	11.45	1.057^a	4.452	< 1.3	34.655 ± 0.005
S 1001	12.40	0.990^b	4.441	< 1.3	33.381 ± 0.008
S 1010	10.48	1.110	4.603	< 1.3	33.950 ± 0.004
S 1016	10.30	1.260	4.596	< 1.3	34.803 ± 0.004
S 1074	10.59	1.120	4.621	< 1.3	33.938 ± 0.003
S 1221[m]	10.76	1.130	4.532	< 1.3	30.372 ± 0.004
S 1231	12.93	0.917	4.381	< 1.3	32.869 ± 0.011
S 1239	12.75	0.758	4.677	2.9 ± 0.7	32.546 ± 0.013
S 1250[m]	9.69	1.360	4.722	< 1.3	36.048 ± 0.003
S 1279	10.55	1.120	4.603	< 1.3	33.340 ± 0.004
S 1288	11.33	1.070	4.502	< 1.3	33.172 ± 0.004
S 1293	12.09	1.007	4.713	1.9 ± 0.8	33.585 ± 0.009
S 1305	12.23	0.993	4.856	3.0 ± 0.7	33.218 ± 0.019
S 1316	10.58	1.100	4.615	< 1.3	32.808 ± 0.004
S 1479	10.55	1.100	4.624	< 1.3	34.398 ± 0.004

^{a} Taken from Sagar & Pati (1989).
^{b} Taken from Sanders (1989).
†† Probably a double-lined spectroscopic binary (SB2).
† SB2 system.
^{m} Single-lined spectroscopic system (Mathieu et al. 1990).

and observed I and radii may not be in perfect agreement on the RGB.

We nevertheless believe that the curves in Fig. 5 are very interesting: they show that the subgiant and RGB parts of the observations are well represented by a $I\Omega = C$ law; this implies that other effects influencing the angular momentum evolution, such as internal redistribution or magnetic braking, if present at all, should be not very relevant for these stars.

On the other hand, it is clear that the region of the turnoff cannot be reproduced by such a law: for $I\Omega = C$ the decrease of rotation predicted between the phases around the turnoff hook is negligible, at odds with the observations. A much steeper law, such as $I\Omega^{0.5} = C$ is required, but this would slow down too much the stars along the subgiant branch.

A possible solution is that the stars in different regions of the C-M diagram do not obey the same angular momentum evolution laws, indicating that their rotation can be governed by different phenomena. For instance we could argue that at the turn-off (where the stars are spending about 1 Gyr), 1.2 $M_\odot$ stars still are undergoing some considerable magnetic braking, which increases their spinning down with respect to angular momentum conservation, while this does not happen anymore in the subgiant and giant phases.

We have indeed some hints that main sequence braking may happen on the main sequence for 1.2 $M_\odot$ stars: for instance the two stars slightly below the turn-off of NGC 3680 ($\sim$1.6 Gyrs) have colors close to $(B-V)_0 = 0.45$, and measured $V \sin i$ of 15.5 and 27.1 km s^{-1} (E30 and 3012, Nordström et al. 1997). This indicates that in $\sim$2.5 Gyrs 1.2 $M_\odot$ stars may spin down considerably, by a factor $\sim$3 ($21.3 \times (4/\pi)/8.53$) with respect to the turnoff stars of M 67 and a factor $\sim$5 if the post turn-off M 67 stars are considered. A similar comparison can made by considering Hyades stars ($\sim$0.7 Gyrs) in the range of effective temperatures between 6450 and 6650 K (corresponding to the range in mass of the M 67 turnoff stars). In this case, even if a strong gradient in rotational velocities is present in this range of colors, the rotational velocities in this cluster are comprised between 25 and 50 km s^{-1} (Gaigé 1993); this is confirmed by CORAVEL $V \sin i$ measurements for 8 stars with $0.42 < (B-V) < 0.47$, which give a mean rotational velocity of 44.4 km s^{-1} (Udry, private communication). Thus, a spin-down of a factor $\sim$5 occurs in $\sim$3.5 Gyrs. It appears therefore that evidence exists for the case of declining velocities of 1.2 $M_\odot$ stars on the main sequence.

It is interesting to note that the main sequence spinning down of 1.2 $M_\odot$ stars may have interesting consequences for understanding the mechanism of Li destruction in the Li gap (Boesgaard 1987), since these stars are indeed in the mass range where this is observed (Deliyannis et al. 1997; Pasquini et al. 2001, in prep.). It is also worth noticing that among the NGC 3680 single turnoff stars (which are a bit more massive than the M 67 ones), and among the Hyades stars the spread in rotational velocities is much larger than the one measured in M 67 (Nordström et al. 1997). We need more stars to further investigate this point, which, if confirmed, would show that the mechanism slowing down main sequence stars tends to produce a uniform distribution.

We can therefore conclude that there is evidence that main sequence 1.2 $M_\odot$ stars spin down during their main sequence, probably via magnetic braking. This spin down continues (or is even more effective) until the star pass the turnoff, then along the subsequent phases the star evolves with a law close to the angular momentum conservation. A crude estimate of main sequence braking is given based on the values quoted above. Rotational velocities should be reduced by a factor $\sim$3 in $\sim$2.5 Gyrs what gives $\sim$1.2/Gyr (from NGC 3680 to M 67) and by a factor $\sim$5 in $\sim$3.5 Gyrs what gives a factor $\sim$1.4/Gyr (from Hyades to M 67). Thus, the rotational velocity at a time t between the Hyades and M 67 for stars of 1.2 $M_\odot$ can be estimated as $V(t)/V_{\text{Hyades}} \sim 0.75/\Delta t$, where $\Delta t = t - t_{\text{Hyades}}$ and t_{Hyades} is the age of the Hyades.

Clearly, the current status of the observations does not allow us anything more than this crude estimate of the braking rate which is, nonetheless, an interesting result for the following reason. The existing data on even younger clusters like the Pleiades and Alpha Per also show a large spread for the observed $V \sin i$, ranging from $\sim$20 to more than 100 km s^{-1} in this $(B-V)$ interval range (Bouvier 1997 and references therein). It appears therefore that evidence exists for the case of declining velocities of 1.2 $M_\odot$ stars on the main sequence. We think that this case is quite interesting because, while for cooler stars the age-dependence of rotational velocities has been extensively studied (see e.g. Bouvier 1997), in these hotter main sequence F stars it is the first time that such a strong evidence is shown. The interest in these stars stems from the fact that they occupy a region very close to the boundary where the change between *hot stars* and *solar stars* type is occurring; hot stars are supposed not to have a solar-type dynamo (and chromospheres and coronae), and not to brake their rotation on the main sequence; 1.2 $M_\odot$ stars instead are in many aspects behaving as "solar stars" also in terms of main sequence braking.

5. Conclusions

In this work we have produced a calibration which allows us to derive an accurate projected rotational velocity $V \sin i$ with the FEROS spectrograph for F-K dwarf and giant stars.

We have applied this technique to 28 stars belonging to the $\sim$4 Gyrs old open cluster M 67. We find that all the observed stars show a very regular rotational pattern, depending on their position on the C-M diagram.

Early G $(0.53 < (B-V)_0 < 0.60)$ main sequence stars rotate about 2 times faster than the Sun, and they show a possible trend with color, in the sense that redder stars seem to rotate slower than bluer ones.

The fastest rotators are 1.2 $M_\odot$ turn-off stars which show a rotational velocity of $\sim$8.5 km s^{-1}; on the other hand, just above the turn-off, the stars are substantially spun down. Rotation declines along the SGB and RGB, and for stars redder than $(B-V) \sim 1$ only upper limits can be found.

By using existing $V \sin i$ determinations in NGC 3680 and the Hyades, the M 67 data can be semi-quantitatively interpreted as an evidence that 1.2 $M_\odot$ stars suffer of extra braking along the main sequence (with a rate of $V(t)/V_{\text{Hyades}} \sim 0.75/\Delta t$ between the Hyades and M 67 ages). The comparison with simple angular momentum laws as derived from theoretical models shows that, while along the RGB M 67 stars evolve close to an angular momentum conservation law $I\Omega = C$, at the tip of the turnoff a stronger braking is required to match the observations. The fact that these stars are suffering MS braking is interesting also in connection with the fact that they belong to the "Lithium dip", a feature which still lacks a firm explanation, and for which angular momentum history has often been invoked as a cause (Deliyannis et al. 1997; Charbonnel & Talon 1999).

References

Allain, S. 1997, Ph.D. Thesis

Baliunas, S. L., & Vaughan, A. H. 1985, ARA&A, 23, 379

Baranne, A., Mayor, M., & Poncet, J. L. 1979, Vistas Astron., 23, 316

Baranne, A., Queloz, D., Mayor, M., et al. 1996, A&AS, 119, 390

Benz, W., & Mayor, M. 1984, A&A, 138, 183

Boesgaard, A. M. 1987, PASP, 99, 1070

Boesgaard, A. M., & Friel, E. D. 1990, ApJ, 351, 491

Bouchy, F., Pepe, F., & Queloz, D. 2001, A&A, submitted

Bouvier, J. 1997, Memorie della Societa Astronomica Italiana, 68, 881

Carraro, G., Girardi, L., Bressan, A., & Chiosi, C. 1996, A&A, 305, 849

Cayrel de Strobel, G., Soubiran, C., Friel, E. D., Ralite, N., & Francois, P. 1997, A&AS, 124, 305

Charbonnel, C., & Talon, S. 1999, A&A, 351, 635

Covino, E., Catalano, S., Frasca, A., et al. 2000, A&A, 361, L49

Deliyannis, C. P., King, J. R., & Boesgaard, A. M. 1997, in Wide Field Spectroscopy, ed. E. Kontzias, 201

Deliyannis, C. P., Pinsonneault, M. H., & Charbonnel, C. 2000, in The Light Elements and their Evolution, ed. L. Da Silva, M. Spite, & J. R. De Medeiros, IAU Symp., 198, 61 (PASP)

De Medeiros, J. R., & Mayor, M. 1999, A&AS, 139, 460

Do Nascimento, J. D., Charbonnel, C., Lèbre, A., de Laverny, P., & De Medeiros, J. R. 2000, A&A, 357, 937

Dubath, P., Meylan, G., Mayor, M., & Magain, P. 1990, A&A, 239, 142

Donahue, R. A., Saar, S. H., & Baliunas, S. L. 1996, ApJ, 466, 348

Dupree, A. K., Whitney, B. A., & Pasquini, L. 1999, ApJ, 520, 751

Fekel, F. 1997, PASP, 109, 514

Gaigé, Y. 1993, A&A, 269, 267

Girard, T. M., Grundy, W. M., Lopez, C. E., & van Altena, W. F. 1989, AJ, 98, 243

Girardi, L., Bressan, A., Bertelli, G., & Chiosi, C. 2000, A&AS, 141, 371

Gray, D. F. 1989, ApJ, 347, 1021

Gray, D. 1976, The Observation and Analysis of Stellar Photosphere (Wiley & Sons, Inc.)

Jones, B. F., Fischer, D., & Soderblom, D. R. 1999, AJ, 117, 338

Kaufer, A., Stahl, O., Tubbesing, S., et al. 1999, The ESO Messenger, 95, 8

Marcy, G. W., & Butler, R. P. 1992, PASP, 104, 277

Mathieu, R. D. 1983, Ph.D. Thesis California Univ., Berkeley

Mathieu, R. D., Latham, D. W., & Griffin, R. F. 1990, AJ, 100, 1881

Mathieu, R. D., Duquennoy, A., Latham, D. W., et al. 1992, in Binaries as Tracers of Stellar Formation, ed. A. Duquennoy & M. Mayor (Publisher, Cambridge University Press, Cambridge, UK, New York, NY), 1992, 278

Mayor, M., & Queloz, D. 1995, Nature, 378, 355

Montgomery, K. A., Marschall, L. A., & Janes, K. A. 1993, AJ, 106, 181

Nordström, B., Andersen, J., & Andersen, M. I. 1997, A&A, 322, 460

Noyes, R. W., Hartmann, L. W., Baliunas, S. L., Duncan, D. K., & Vaughan, A. H. 1984, ApJ, 279, 777

Pallavicini, R., Golub, L., Rosner, R., et al. 1981, ApJ, 248, 290

Pasquini, L., & Belloni, T. 1998, A&A, 336, 902

Pasquini, L., Randich, S., & Pallavicini, R. 1997, A&A, 325, 535

Pasquini, L., De Medeiros, J. R., & Girardi, L. 2000, A&A, 361, 1011

Peterson, R. C. 1985, ApJ, 297, 309

Queloz, D., Allain, S., Mermilliod, J.-C., Bouvier, J., & Mayor, M. 1998, A&A, 335, 183

Sagar, R., & Pati, A. K. 1989, BASI, 17, 6

Sanders, W. L. 1977, A&AS, 27, 89

Sanders, W. L. 1989, RMxAA, 17, 35

Setiawan, J., Pasquini, L., Da Silva, L., et al. 2000, The Messenger, 102, 13

Shetrone, M. D., & Sandquist, E. L. 2000, AJ, 120, 1913

Taylor, B. J. 1999, A&AS, 139, 68